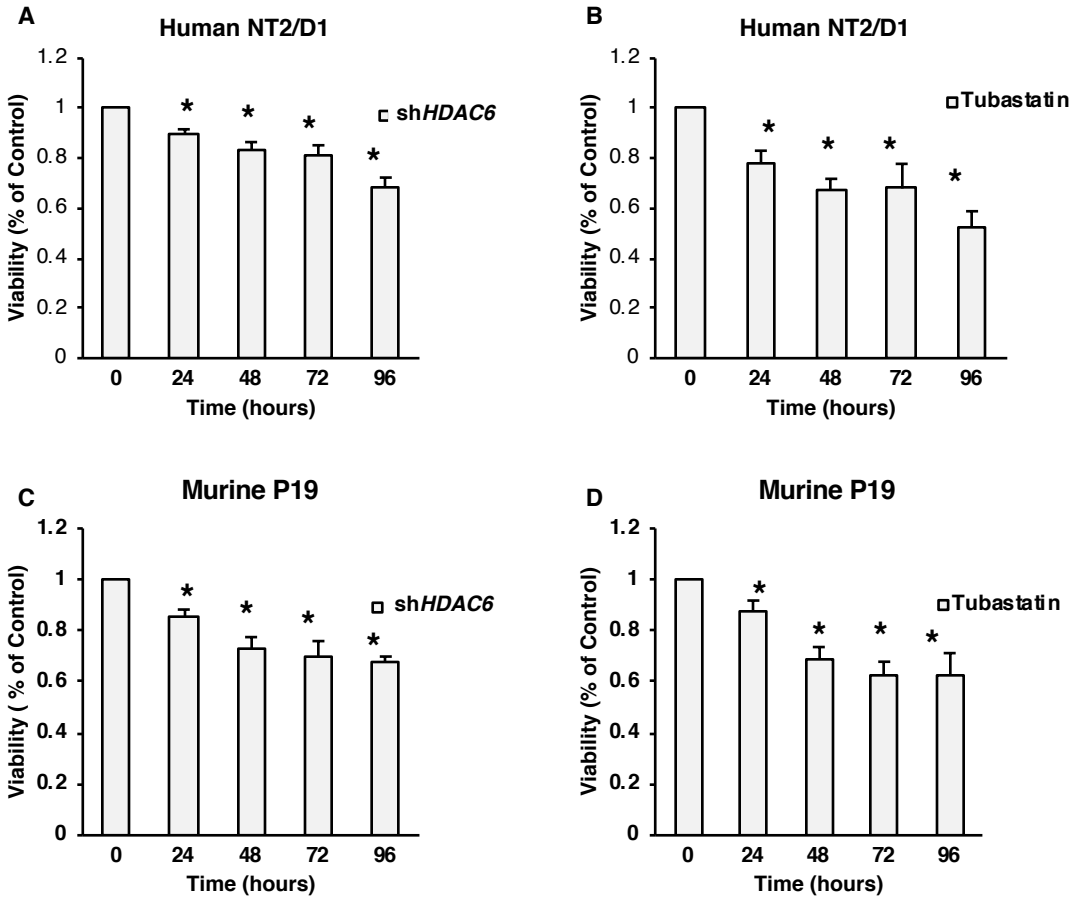

Figure S1. HDAC6 inhibition decreases the viability of NT2/D1 and P19 cancer stem cells (CSCs). (**A and B**) NT2/D1 tubastatin A-treated and HDAC6 KD cells were stained with MTS reagent and the percentage of proliferation was determined after 24, 48, 72 and 96 h. (**C and D**) P19 tubastatin A-treated and HDAC6 KD cells were stained with MTS reagent and the percentage of proliferation was determined after 24, 48, 72 and 96 h.

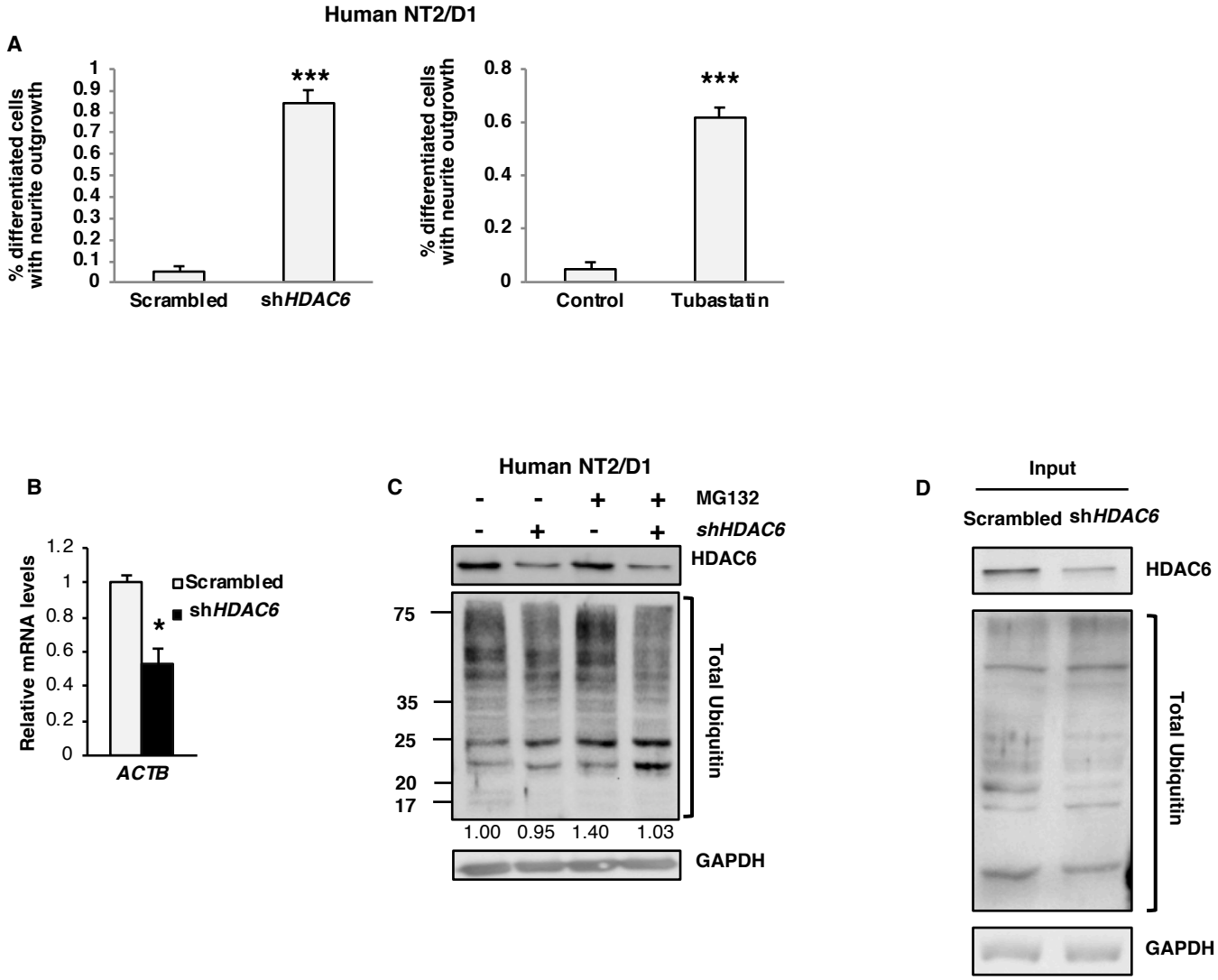

Figure S2. HDAC6 inhibition promotes differentiation and increases the stability of ACTB/β-actin. (**A**) NT2/D1 tubastatin A-treated and HDAC6 KD cells were analyzed by microscopy for morphological changes and the percentage of cells displaying neurite outgrowths were quantified using ImageJ software. (**B**) NT2/D1 HDAC6 KD cells were subjected to qRT-PCR analysis for differentiation factor ACTB. (**C**) NT2/D1, HDAC6 KD cells treated with or without MG132 for 4 h were subjected to WB analysis for total ubiquitin. The numbers below the blot correspond to densitometry quantification of blots normalized to the loading control. (**D**) NT2/D1 HDAC6 KD cells were subjected to immunopreciptiation for ACTB and the input samples we subjected to WB analysis for HDAC6 and total ubiquitin.

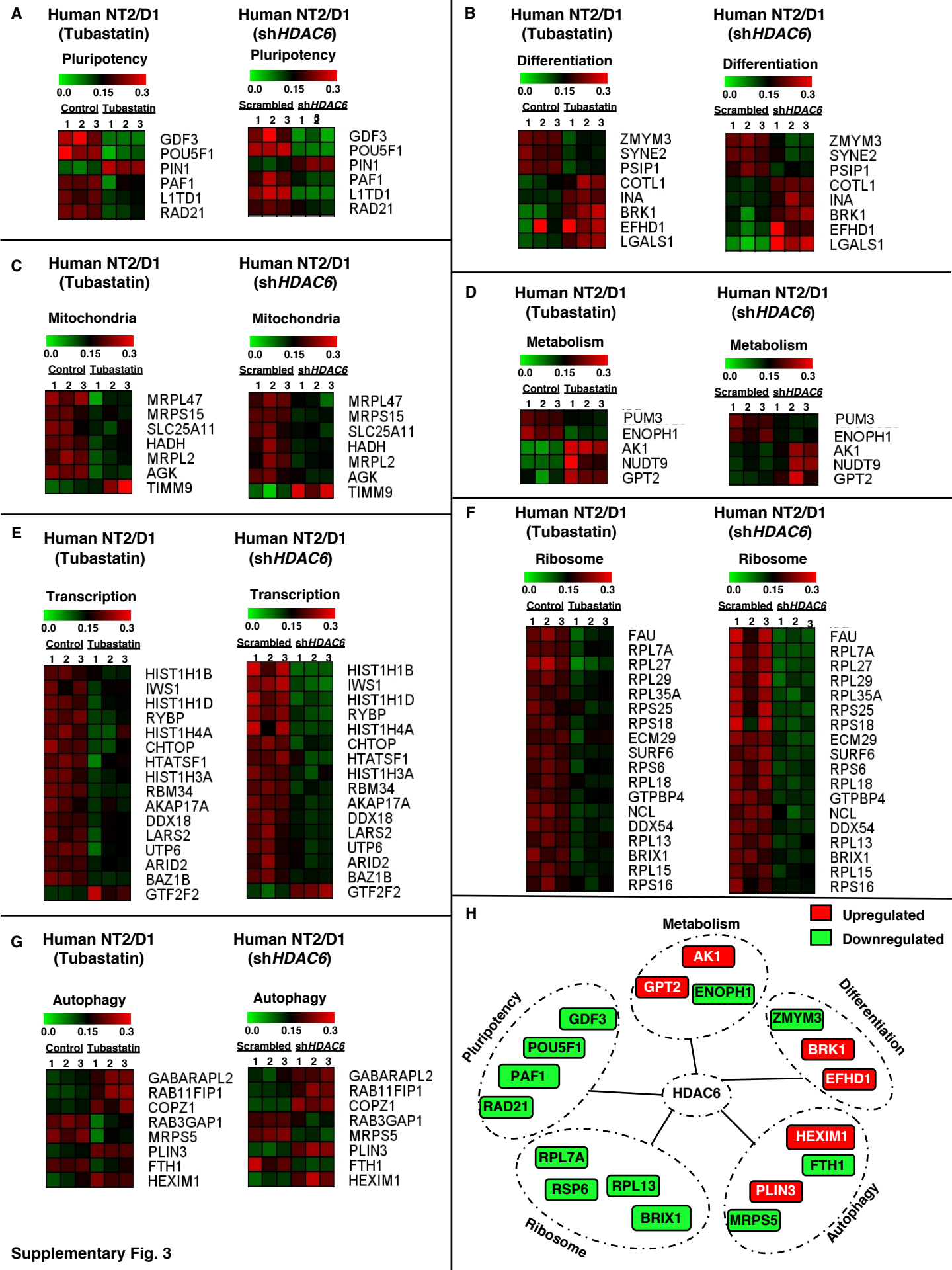

Supplementary Fig. 3

Figure S3. Global proteome analysis of NT2/D1 cancer stem cells (CSCs) following HDAC6 inhibition. (**A and B**) Heat maps comparing the proteomic analysis of pluripotency- and differentiation-related proteins in tubastatin A-treated or HDAC6 KD NT2/D1 cells. (**C and D**) Heat map comparing the proteomic analysis of mitochondria- and metabolism -elated proteins in tubastatin A-treated or HDAC6 KD NT2/D1 cells. (**E and F**) Heat map comparing the proteomic analysis of transcription- and ribosomal-related proteins in tubastatin A-treated or HDAC6 KD NT2/D1 cells. (**G**) Heat map comparing the proteomic analysis of autophagy-related proteins in tubastatin A-treated or HDAC6 KD NT2/D1 cells. (**H**) Graphical depiction of examples of selected proteins related to pluripotency, metabolism, differentiation, autophagy and ribosome which are either upregulated (red) or downregulated (green) by both HDAC6 KD and inhibition.

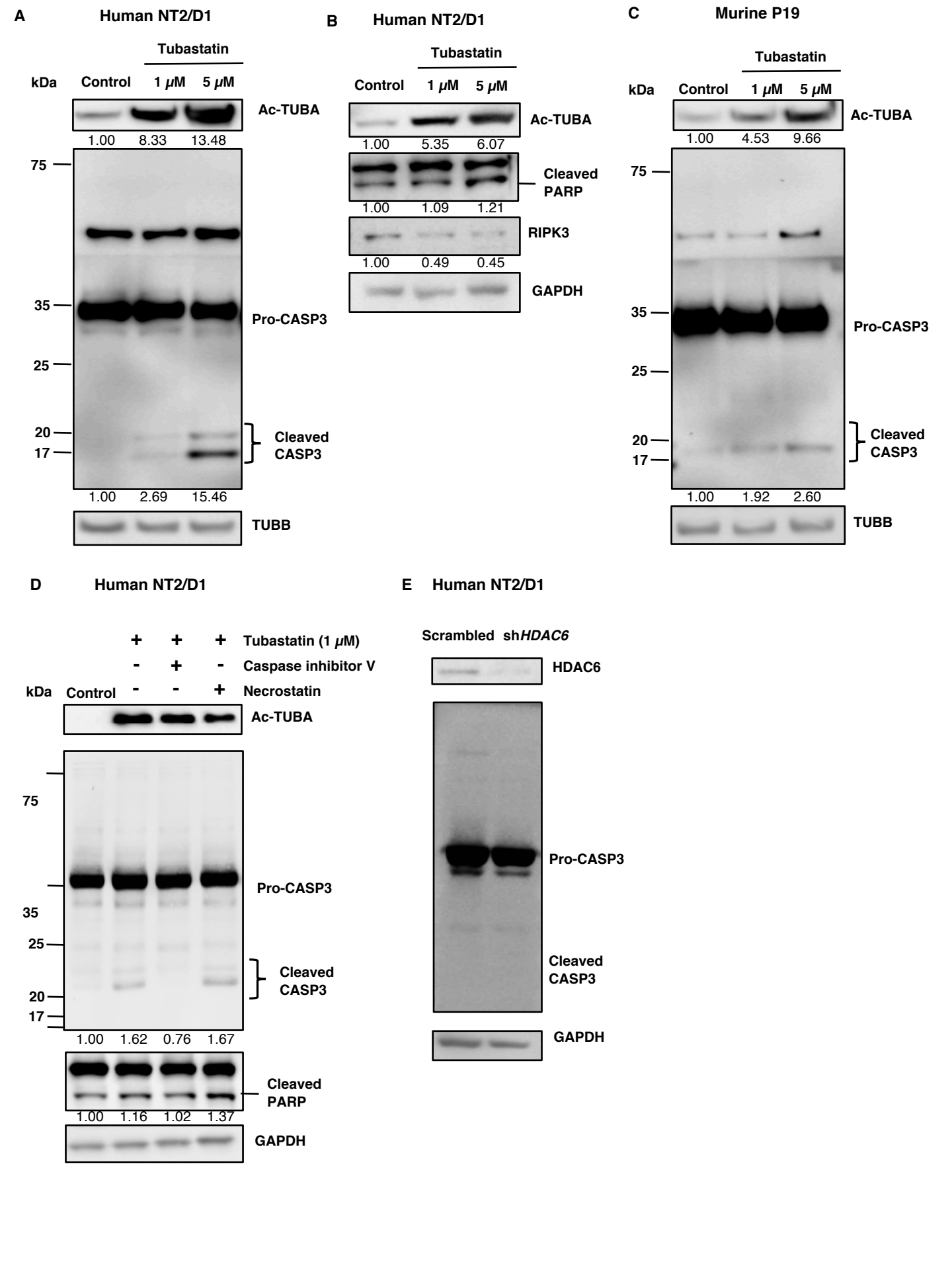
A
Human NT2/D1
Tubastatin
kDa
Control
1 μM
5 μM
Ac-TUBA
1.00
8.33
13.48
75
35
25
20
17
Pro-CASP3
Cleaved CASP3
1.00
2.69
15.46
TUBB
B
Human NT2/D1
Tubastatin
Control
1 μM
5 μM
Ac-TUBA
1.00
5.35
6.07
Cleaved PARP
1.00
1.09
1.21
RIPK3
1.00
0.49
0.45
GAPDH
C
Murine P19
Tubastatin
kDa
Control
1 μM
5 μM
Ac-TUBA
1.00
4.53
9.66
75
35
25
20
17
Pro-CASP3
Cleaved CASP3
1.00
1.92
2.60
TUBB
D
Human NT2/D1
+ + + Tubastatin (1 μM)
- + - Caspase inhibitor V
- - + Necrostatin
kDa
Control
Ac-TUBA
75
35
25
20
17
Pro-CASP3
Cleaved CASP3
1.00
1.62
0.76
1.67
Cleaved PARP
1.00
1.16
1.02
1.37
GAPDH
E
Human NT2/D1
Scrambled
sh*HDAC6*
HDAC6
Pro-CASP3
Cleaved CASP3
GAPDH

Figure S4. HDAC6 inhibitor-mediated effect on pluripotency and differentiation of CSCs is independent of CASP3. (**A and B**) NT2/D1 cells were treated with tubastatin A and subjected to WB for (**A**) Pro-CASP3 and cleaved CASP3, (**B**) cleaved PARP and RIPK3. The numbers below the blots correspond to densitometry quantification of blots normalized to the loading control. (**C**) P19 cells were treated with tubastatin A and subjected to WB for Pro-CASP3 and cleaved CASP3. (**D**) NT2/D1 cells were pre-treated with caspase inhibitor V or necrostatin followed by treatment with tubastatin A and subjected to WB for Pro-CASP3 and cleaved CASP3, and cleaved PARP. (**E**) NT2/D1 HDAC6 KD cells were subjected to WB for Pro-CASP3 and cleaved CASP3.

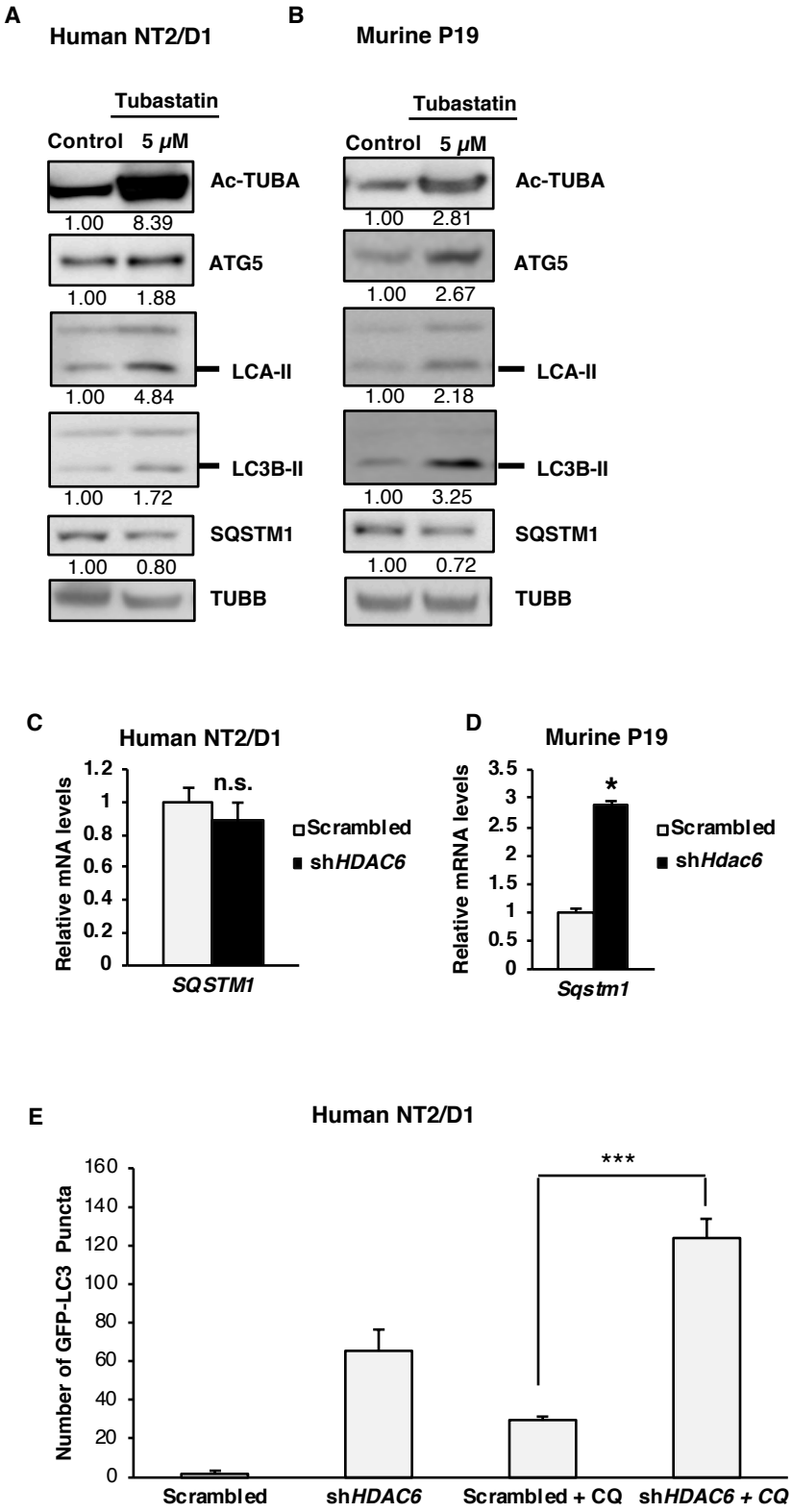

Figure S5. HDAC6 inhibition promotes autophagy in NT2/D1 and P19 cancer stem cells (CSCs). (**A**) Tubastatin A-treated NT2/D1 and (**B**) P19 cells were subjected to WB analysis for ATG5, LC3A-II, LC3B-II and SQSTM1. (**C and D**) qRT-PCR analysis for *SQSTM1*/*Sqstm1* in (**C**) NT2/D1 HDAC6 KD and (**D**) P19 HDAC6 KD cells. (**E**) NT2/D1 HDAC6 KD cells were transfected with GFP-LC3-overexpressing plasmid and treated with chloroquine (CQ), and puncta formation was analyzed by confocal microscopy and quantified using ImageJ software.

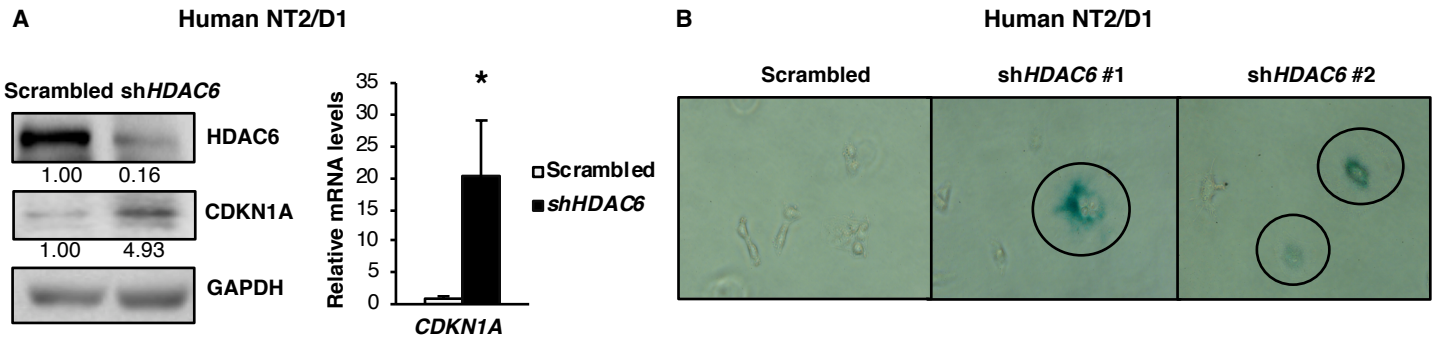

Figure S6. HDAC6 inhibition promotes senescence in NT2/D1 cancer stem cells (CSCs). (**A**) WB and qRT-PCR analysis for CDKN1A/p21 in NT2/D1 HDAC6 KD cells. (**B**) NT2/D1 HDAC6 KD cells were labelled with GLB1/b-galactosidase to detect senescence. Statistical analysis was performed with two-tailed, Student's *t*-test with 95% confidence interval; *P-values < 0.05 obtained by comparing the respective data with the scrambled control. Not in the current Fig. S6.

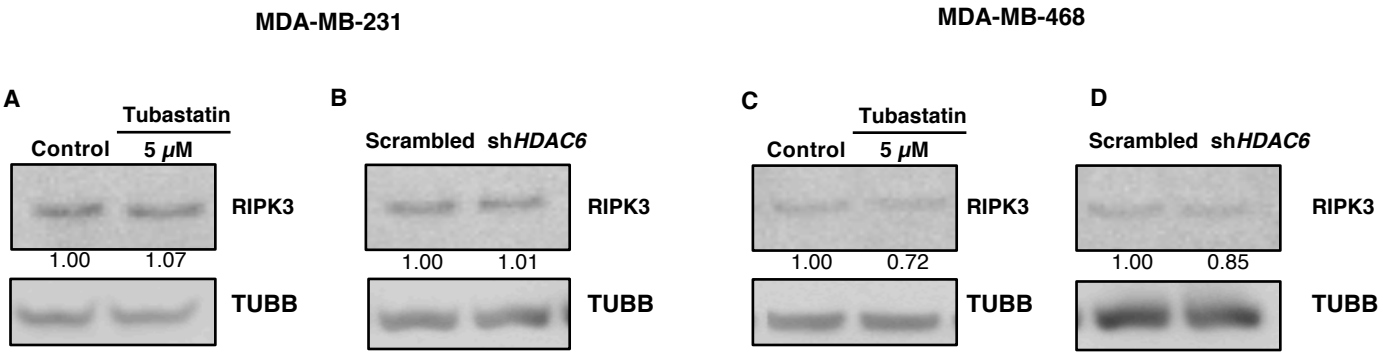

Figure S7. HDAC6 inhibition does not promote necroptosis in MDA-MB-231 and MDA-MB-468 breast cancer cells. MDA-MB-231 treated with tubastatin A (**A**) or HDAC6 KD (**B**) were subjected to western blot analysis for RIPK3. MDA-MB-468 treated with tubastatin A (**C**) or HDAC6 KD (**D**) were subjected to WB analysis for RIPK3.

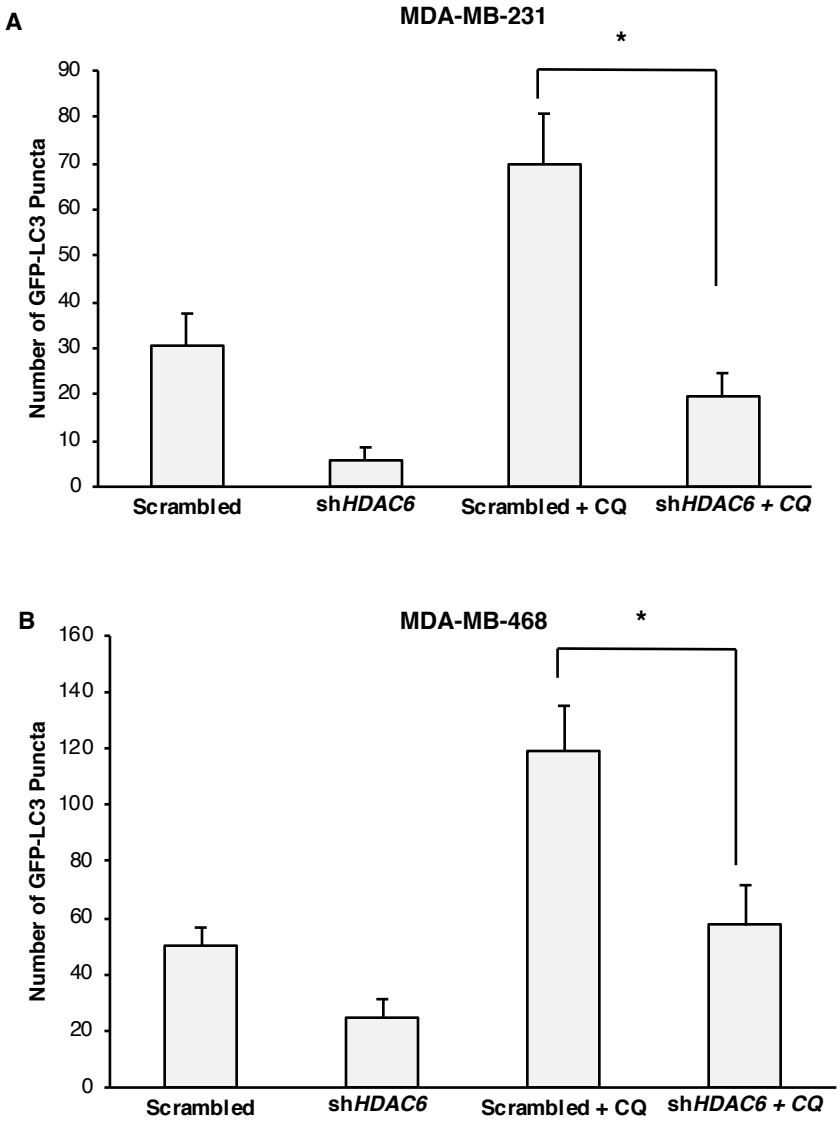

Figure S8. HDAC6 inhibition does not upregulate autophagy in MDA-MB-231 and MDA-MB-468 breast cancer cells. (**A**) MDA-MB-231 or (**B**) MDA-MB-468 HDAC6 KD cells were transfected with GFP-LC3-overexpressing plasmid and treated with chloroquine (CQ) and puncta formation was analyzed by confocal microscopy and quantified using ImageJ software.

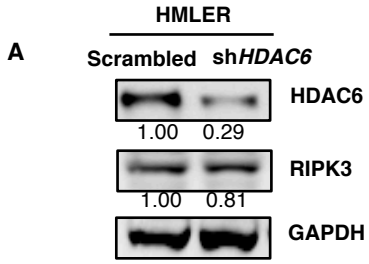

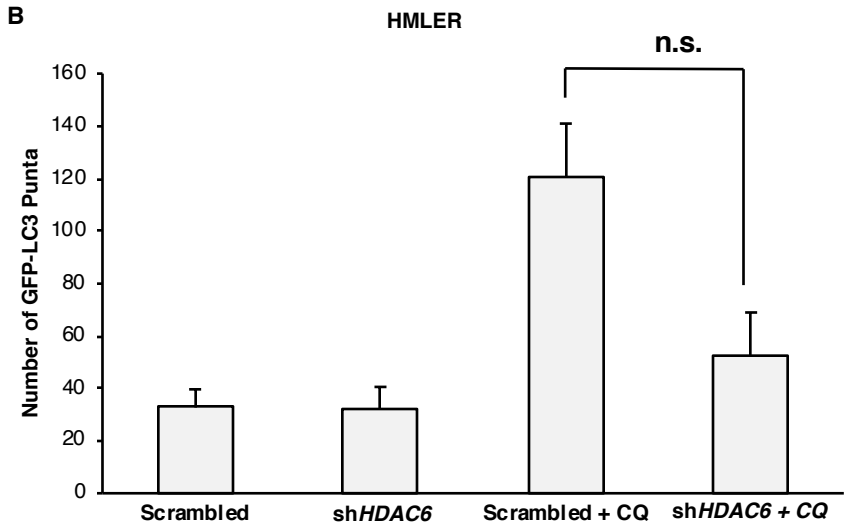

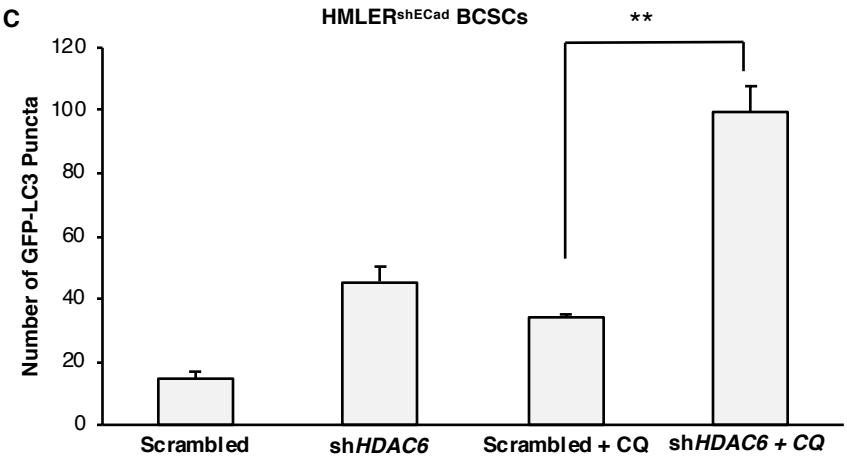

Figure S9. HDAC6 KD does not promote necroptosis and differentially regulates autophagy in differentiated HMLER breast cancer cells and HMLER^{shECad} breast cancer stem cells (BCSCs). (**A**) HMLER breast cancer cells with HDAC6 KD were subjected to western blot analysis for RIPK3. Numbers below the blots correspond to densitometry quantification of blots normalized to the loading control. (**B**) HMLER or (**C**) HMLER^{shECad} Breast cancer stem cells (BCSCs) HDAC6 KD cells were transfected with GFP-LC3-overexpressing plasmid and treated with chloroquine (CQ) and puncta formation was analyzed by confocal microscopy and quantified using ImageJ software. n.s., not significant; **, *P*-values < 0.005.

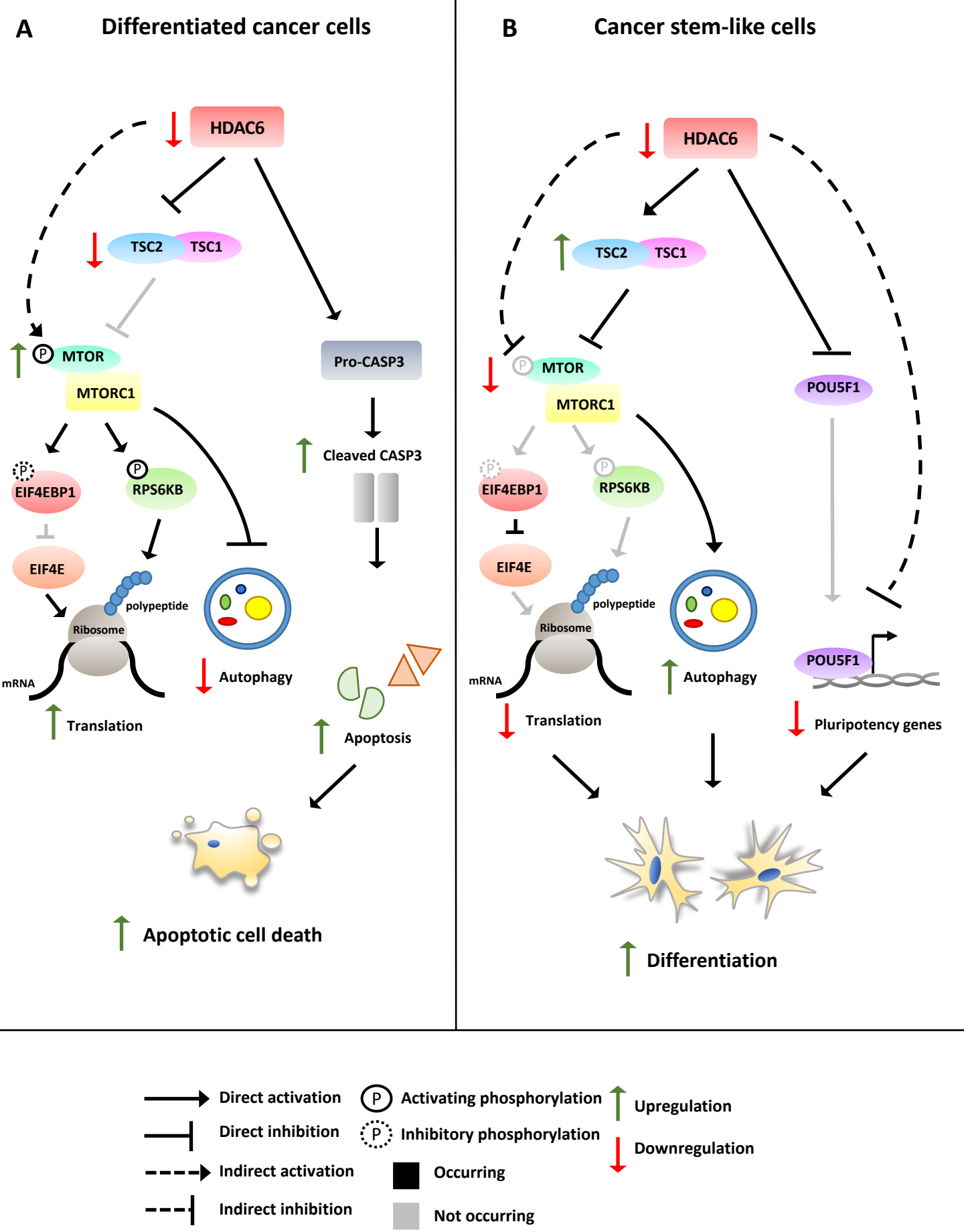
A
Differentiated cancer cells
HDAC6
TSC2
TSC1
MTOR
MTORC1
Pro-CASP3
Cleaved CASP3
EIF4EBP1
RPS6KB
EIF4E
polypeptide
Ribosome
mRNA
Autophagy
Translation
Apoptosis
Apoptotic cell death
B
Cancer stem-like cells
HDAC6
TSC2
TSC1
MTOR
MTORC1
POU5F1
EIF4EBP1
RPS6KB
EIF4E
polypeptide
Ribosome
mRNA
Autophagy
POU5F1
Translation
Pluripotency genes
Differentiation
Direct activation
Direct inhibition
Indirect activation
Indirect inhibition
Activating phosphorylation
Inhibitory phosphorylation
Occurring
Not occurring
Upregulation
Downregulation

Figure S10. HDAC6 differentially regulates autophagy and apoptosis in CSCs and differentiated breast cancer cells. (**A**) HDAC6 KD in differentiated breast cancer cells decreases the levels of the tuberous sclerosis tumor suppressor complex, TSC1 and TSC2. This increases the levels of phosphorylated MTOR and inhibits autophagy. HDAC6 KD also increases the levels of cleaved CASP3, leading to increased apoptotic cell death. (**B**) HDAC6 KD in CSCs increases the levels of members of the tuberous sclerosis tumor suppressor complex, TSC1 and TSC2. This decreases the levels of phosphorylated MTOR and increases autophagy. This also decreases the phosphorylation of the downstream targets of p-MTOR signaling, EIF4EBP1 and RPS6KB, which inhibits protein translation. HDAC6 KD also decreases the levels of the master pluripotency transcription factor, POU5F1, resulting in the inhibition of pluripotency and the promotion of differentiation in CSCs.